Aquaculture 318 (2011) 412–424

Contents lists available at ScienceDirect

Aquaculture

journal homepage: www.elsevier.com/locate/aqua-online

A physical–biological coupled aquaculture model for a suspended aquaculture area of China

Jie Shi [a,c,*], Hao Wei [b,c], Liang Zhao [c], Ye Yuan [c,d], Jianguang Fang [e], Jihong Zhang [e]

[a] Key Laboratory of Marine Environment & Ecology, Ministry of Education, Ocean University of China, Qingdao 266100, China
[b] College of Marine Science and Engineering, Tianjin University of Science & Technology, Tianjin 300457, China
[c] Lab of Physical Oceanography, Ocean University of China, Qingdao 266100, China
[d] National Marine Environmental Forecasting Center, State Ocean Administration, Beijing, China
[e] Key Laboratory for Sustainable Utilization of Marine Fisheries Resource, Yellow Sea Fisheries Research Institute, Chinese Academy of Fishery Science, Qingdao 266071, China

ARTICLE INFO

Article history:
Received 8 August 2010
Received in revised form 29 May 2011
Accepted 30 May 2011
Available online 12 June 2011

Keywords:
Suspended aquaculture
Aquaculture drags
Surface boundary layer
Physical–biological coupled aquaculture model

ABSTRACT

A three-dimensional physical–biological coupled aquaculture model is developed to study the aquaculture carrying capacity of kelp in Sungo Bay, a typical aquaculture site in China with intensive suspended raft aquaculture. In the aquaculture model, the hydrodynamic module builds on the Princeton Ocean Model by adding two types of drags due to the aquaculture facilities at surface and kelp in water column. The biological module simulates the renewal of dissolved inorganic nitrogen (DIN), the cycle of phytoplankton biomass, and the growth of kelp, while the contribution of bivalves' excretion to DIN is set to a constant derived from observations. Thus, the coupling between the growth of kelp and the current variation can be studied by adding drags in the layers reached by kelp. The simulated magnitude and vertical profile of currents agree well with observations. The suspended aquaculture causes a reduction in the average speed of surface current by 40%, decreasing the water exchange with the open sea. The simulation results also show that the seasonal and spatial variations of the DIN concentration and phytoplankton biomass are clearly controlled by the distributions of different species. The estimation of DIN budgets of different periods shows competition between kelp and phytoplankton. The primary source of nutrients for the growth of kelp in Sungo Bay is the DIN from the open sea, and the aquaculture obstruction is the main reason for the deficient DIN in the kelp culture area. The final kelp production decreases from the mouth to the end of the bay, consistent with the spatial variation of water exchange rate. Numerical experiments have been carried out by increasing the aquaculture density of kelp from 0.8 to 1.5 times of the current value. Obtained results indicate that the optimal average density is 0.9 times of the current value.

1. Introduction

Fisheries and aquaculture are both important ways of seafood production in China. For example, the consumption of seafood in 2008 in China was 25 million tons and the predicted demand will reach about 40 million tons in 2020. However, marine fish stocks are decreasing in the last decades. The increasing demand of seafood production will rely more on aquaculture and the intensive aquaculture could be an important method to address the challenge. Considered that aquaculture production in a coastal bay is limited, a sustainable aquaculture method needs to be established for supporting a long-term and stable supply. In 1934, Errington first introduced the concept of "carrying capacity" to aquaculture (Kashiwai, 1995) that was also applied to administration of water quality and tourism, etc. (Duarte et al., 2003). With respect to aquaculture, carrying capacity is described as the standing stock at which the annual production of the marketable cohort is maximized (Bacher et al., 1998). Accurate estimation of the carrying capacity is an important step for sustainability in aquaculture.

Suspended aquaculture is popular in semi-closed bays with aquaculture activities in China. Kelp and bivalves could grow in cages, nets, or other containers hung from floats or rafts. Thus, suspended aquaculture can be considered as an integrated system that includes the cultivated species, facilities (buoys, ropes and rafts) and the environment. Various types of ecosystem models have been developed to estimate the carrying capacity of such systems. Energy-balanced models are generally based on the balance between depletion and renewal of nutrients and food (Grant, 1996; Wildish and Kristmanson, 1997). For example, Fang et al. (1996a, b) estimated the carrying capacity of kelp and bivalves in Sungo Bay of China (the study area of this work) based on the balance of DIN and organic carbon. These models have two limitations: 1) only single species being considered and 2) the complexity of biological and physical

* Corresponding author at: College of Environmental Science and Engineering, Ocean University of China, 238 Songling Road, Qingdao, Shandong, 266100, China.
E-mail address: shijie@ouc.edu.cn (J. Shi).

0044-8486/$ – see front matter © 2011 Elsevier B.V. All rights reserved.
doi:10.1016/j.aquaculture.2011.05.048

processes being not included. Box models including more complicated biological processes can be used to predict the growth of more than one species and estimate carrying capacity (Grant et al., 2007; Nunes et al., 2003; Raillard and Ménesguen, 1994; Zhu et al., 2002). However, these box models oversimplify the flow and its potentially important interactions with nutrients and food availability for cultivated species. It is not surprising that these models cannot simulate details of flow variability, neither the effects of species and facilities on hydrodynamic.

Generally, flows tend to slow down in suspended aquaculture areas because of the extra drags caused by the suspended system. Based on observations, Grant et al. (1998) estimated that the drag due to the mussel raft aquaculture was about 30 times of that for a bare substrate. Pilditch et al. (2001) observed a reduction by 40% of current passing through suspended scallop aquaculture from the average surrounding values. In New Zealand, Gibbs et al. (1991) estimated that the current within longline mussel aquaculture was about 70% of that in the surrounding areas. Boyd and Heasman (1998) carried out a comprehensive study on the effects of suspended aquaculture on tidal currents. They reported that the current within the rafts depended on rope spacing and current speed and could be reduced by a factor of 6.

Overall, it is important to couple hydrodynamic processes into carrying capacity models. By using a two-dimensional model Grant and Bacher (2001) estimated a reduction by 41% in the water exchange rate by increasing the bottom friction in Sungo Bay with intensive suspended aquaculture. This suggested that neglecting the physical barriers could lead to a significant overestimation of the water exchange rate and the renewal of nutrient and food. The same was true for the aquaculture carrying capacity. Using the same approach, Duarte et al. (2003) found that Sungo Bay was being exploited close to its environmental carrying capacity; however, an optimized distribution of aquaculture may further increase the yield.

The suspended aquaculture causes not only decreases in the magnitude, but also changes in the vertical profile of current. In order to study the hydrodynamics under the influence of aquaculture activities in Sungo Bay, two field campaigns were carried out in April and July 2006 (Fig. 1). Fig. 2 compared the typical vertical profiles of tidal current at station Xunshan in Sungo Bay and at station A1 in the southern Yellow Sea (observed in December 2005) without aquaculture. In April when kelp in Sungo Bay reached its maximum length, the current at the surface layer had only half the magnitude in the middle layer, and led the bottom layer by up to 2 h; the maximum current speed occurred in the lower part of the water column (Fig. 2a). In common area without aquaculture (taking observations at station A1 as an example), the maximum tidal current occurred at the surface and decreased gradually toward the bottom; the bottom current led that at the surface (Fig. 2b). Clearly, the aquaculture activities caused significant changes in current structure in Sungo Bay. The aquaculture-induced drags have both spatial and temporal variations. Spatial variations are caused by horizontal distributions of aquaculture, and temporal variations are caused by the changing kelp length associated with growth.

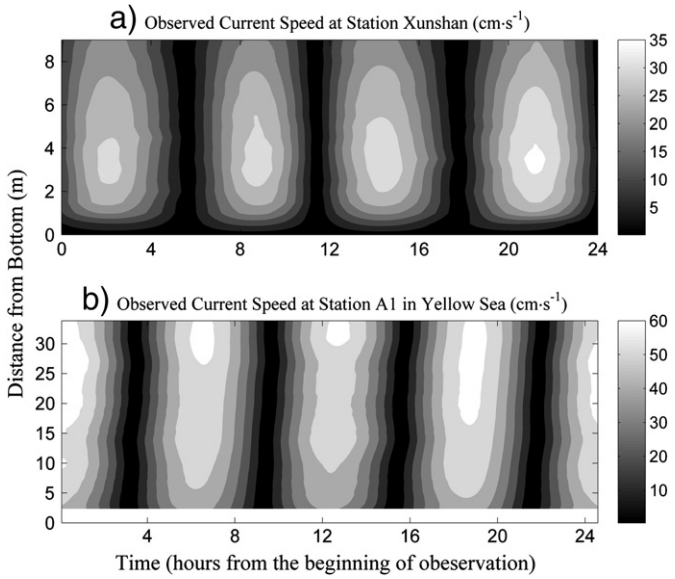

Fig. 2. Observed vertical profiles of tidal current over 25 h at (a) station Xunshan in April 2006 (measured with 500 kHz SONTEK ADP) and (b) station A1 in March 2005 (measured with 600 kHz RD ADCP).

In this study, a three-dimensional model was modified by including two types of drags to study the dynamic coupling between physical and biological processes in Sungo Bay. Accurate magnitude and vertical structure of current were predicted by the model. Reasonable annual cycles of DIN concentration, phytoplankton biomass and kelp production were obtained and discussed.

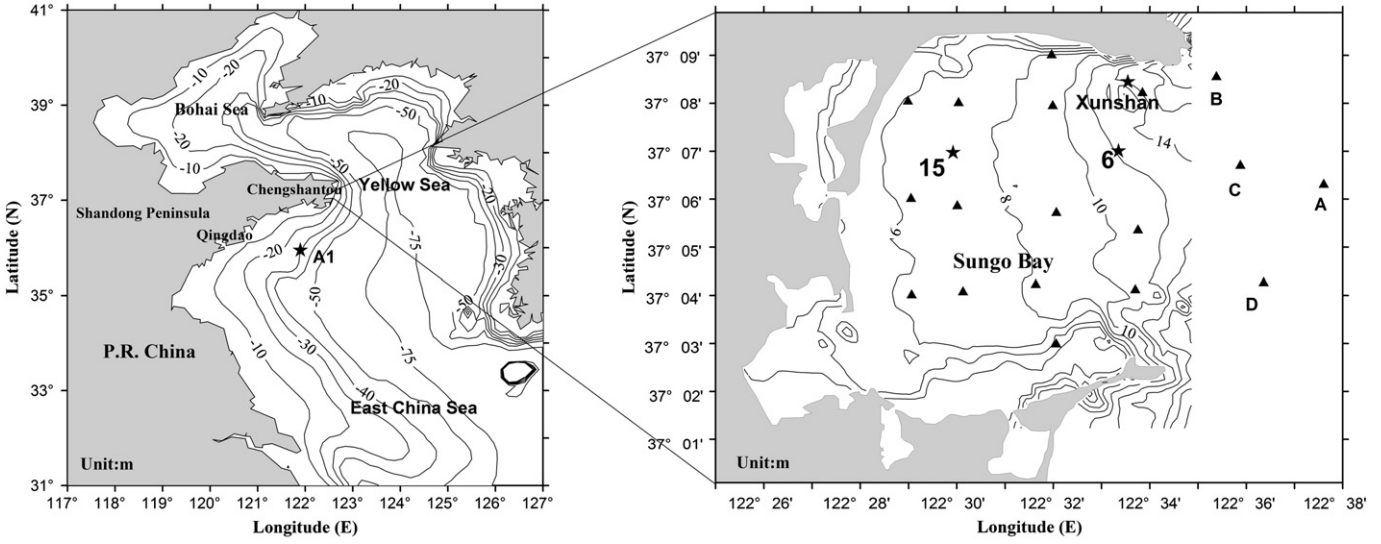

Fig. 1. The location and topography (in m) of the study area. The observational stations are marked by stars. Stations Xunshan, 6 and 15 are located inside Sungo Bay; station A1 is located in the southern Yellow Sea. Observational data at stations within Sungo Bay (marked by triangles) in November, 2006 are used to provide initial conditions of state variables. Data collected at stations A, B, C and D in January, April, July and November of 2006 are used to construct the boundary forcing for the model.

Additionally, kelp carrying capacity in Sungo Bay was estimated by changing aquaculture densities.

2. Methodology

2.1. Study area

Sungo Bay is located at the eastern end of the Shandong Peninsula of China (37°01′–37°09′N, 122°24′–122°35′E), opening to the Yellow Sea. It has an area of 140 km^2, with depths increasing gradually from less than 1 m at the end to approximately 20 m at the mouth of the bay (Fig. 1). It has been used for aquaculture for more than 30 years and is one of the most important aquaculture sites in China. Presently, nearly the whole bay is covered by aquaculture facilities. The main species are kelp (*Laminaria japonica*) and bivalves cultivated in different regions (Fig. 3). Kelp monoculture occurs mainly near the mouth of the bay; bivalves are mainly raised near the end of the bay; the middle part is characterized by kelp-and-bivalve aquacultures (Fang et al., 1996a). Bivalves are mostly raised in cages hung from rafts; and kelp is tied to ropes and grows downward in the water column (Figs. 4 and 5). The annual production of kelp is about 8.0×10^4t in dry weight; and that of bivalves is approximately 1.2×10^5t with shells.

The tidal elevation in Sungo Bay is irregularly semidiurnal with a maximum tidal range of about 2 m. The tidal current is regularly semidiurnal. The flooding tide current enters the bay along the northern side, flows anticlockwise and exits along the southern side; the ebbing tide is in the opposite direction. Nutrients and food, which feed the aquaculture species, are mainly supplied by the exchange with the open sea.

In recent years, aquaculture has been expanded from the bay to the open sea and the aquaculture density has been increased to meet the increasing market demand. Unexpectedly, the total aquaculture production in this area has not increased. Kelp decays at the beginning of the harvest period, and bivalves grow slower and reach smaller sizes. The situation was thought to be associated with the deficient supply of nutrients and food because of the decrease in water exchange resulted from the obstruction of circulation by the increasing aquaculture activities (Fang, et al., 1996c).

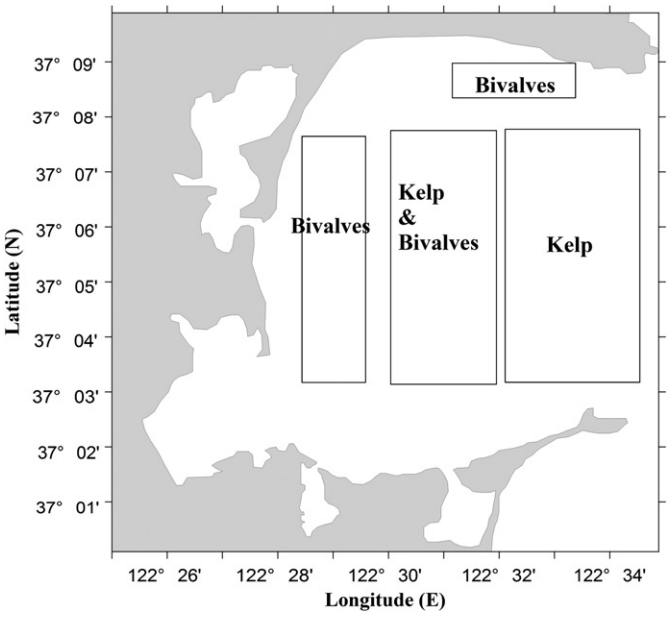

Fig. 3. Aquaculture setup in Sungo Bay, showing the regions of kelp monoculture, bivalve monoculture and multi-species aquaculture, respectively.

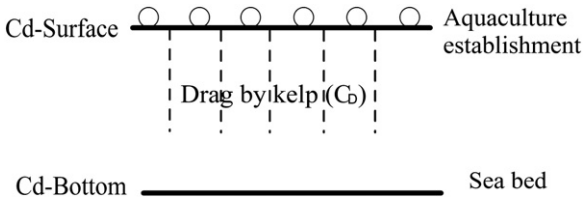

Fig. 4. Schematic side view of culture drags. Open circles represent the aquaculture establishment at the surface (e.g. ropes, buoys and rafts) and dashed lines represent kelp growing from surface down into the water column.

2.2. Hydrodynamic model

The hydrodynamic component is based on the Princeton Ocean Model and modified by adding two types of drags to investigate the influences of high density aquaculture on the hydrodynamic field. One drag is the surface stress due to the facilities, depending on the current speed and the fixed facilities lying at surface throughout the year. The other is the kelp drag force. It depends not only on the current speed but also on the size of kelp, varies significantly in different stages of kelp growth, and could be reduced to zero after the kelp harvest. The drag caused by the facilities is a shear stress analogous to wind stress since the facilities always float at the surface. The drag caused by kelp is a body force added in the water layers that kelp can reach, thus it depends on the length of kelp.

2.2.1. Drag at the surface

Fig. 6 shows the observed vertical structure of current in July 2006, when kelp was nearly completely harvested, but the aquaculture facilities were still present at the surface (in fact throughout the year). The observations suggested that the vertical distribution of the flow in the surface boundary layer (SBL) and bottom boundary layer (BBL) were similar. The logarithmic law-of-the-wall approximately fitted the flow structures in both the BBL and SBL (Fan et al., 2009). Therefore the surface stress is parameterized in the quadratic form similar as the bottom drag, i.e.,

$$\vec{\tau} = \rho\overline{C_{ds}}\left|\vec{U}_s\right|\vec{U}_s$$

where ρ is the water density, $\overline{C_{ds}}$ is the averaged surface drag coefficient and $\vec{U}_s$ is the surface current velocity. The drag coefficient was derived by fitting the vertical profiles of tidal current observed in July 2006 (Fan et al., 2009). The instantaneous surface drag coefficient

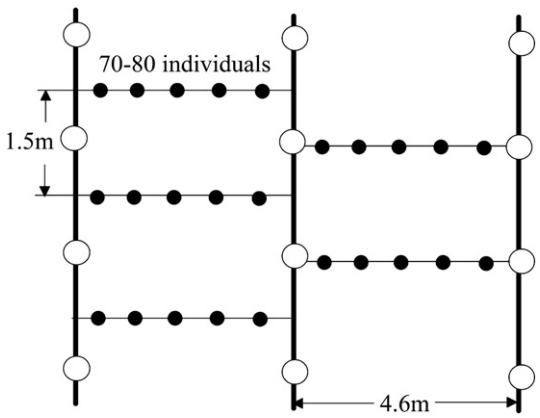

Fig. 5. Top view of the kelp culture at the surface. Thicker lines represent rafts; open circles represent buoys at the surface; thinner lines represent ropes. The kelp individuals (marked by dots) are planted on the ropes and grow downward in the water column.

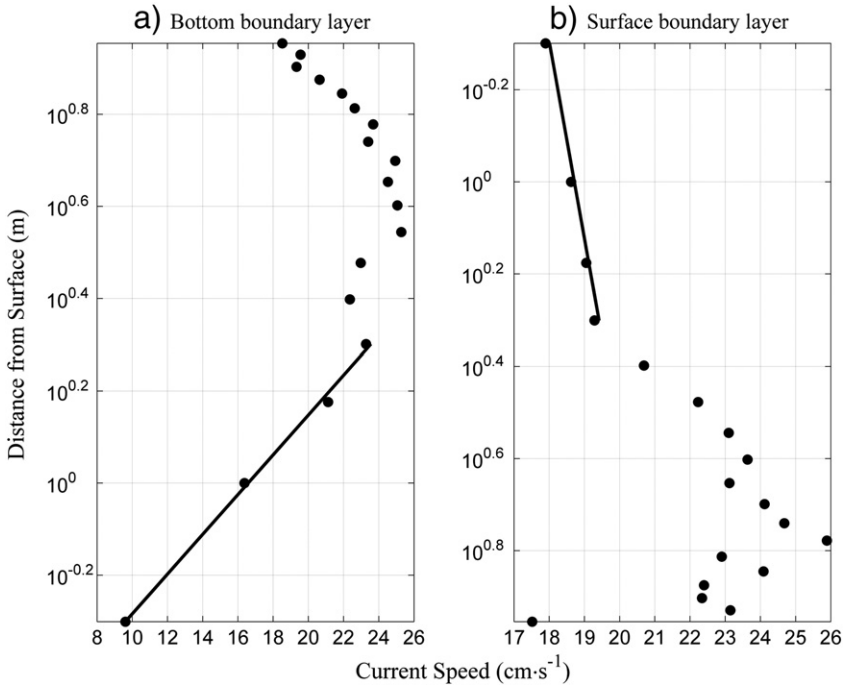

Fig. 6. Vertical profile of tidal current at station Xunsan in July, 2006. The vertical axes are distances from (a) the bottom and (b) the surface, plotted on logarithmic scales. The straight lines represent the fits to the logarithmic law-of-the-wall.

varied within the range between 1.6×10^{-4} and 2.5×10^{-1}. Its average value of 7.0×10^{-2} is used in the model. The surface stress is applied to the whole aquaculture area throughout the whole year.

2.2.2. Drag in the water column

From early November when kelp is seeded to July when it is totally harvested, the water exchange in the water column is significantly influenced by kelp. Jackson and Winant (1983) studied the kelp-induced drag in a kelp forest along the coast of southern California, where kelp was attached to hard substrata and grew upward. A parameterization of the drag per plant was proposed as

$$D_0 = C_d \rho u^2 dl$$

where l was the kelp length, ρ was the water density, d was the diameter of the stipe bundle, u was the velocity and C_d was the drag coefficient (about 0.5 for flow perpendicular to a cylinder) (Bachelor, 1967). In Sungo Bay, kelp is tied to ropes at surface and grows downward. The drag per unit mass is set to

$$\vec{D} = C_D|\vec{u}|\vec{u}$$

where the drag coefficient C_D is set to 0.025 according to the kelp diameter, length, and aquaculture density in Sungo Bay. Horizontally, the kelp-induced drag is added in the regions of kelp monoculture and the multi-species aquaculture. The length of kelp is set to zero on 1st November (when kelp is seeded) and assumes to increase linearly to 5 m on 31st May of the following year (when kelp is harvested). During kelp growth period at each model time step, the length of kelp is calculated for determining the number of vertical grids where this drag force should be applied.

2.3. Aquaculture model

The aquaculture ecosystem component includes four state variables, i.e., the concentrations of the dissolved inorganic nitrogen (DIN), the particulate organic matter (POM) and chlorophyll-a, and the dry weight of kelp. The biogeochemical processes included in the ecosystem component are shown in Fig. 7. Duarte et al. (2003) estimated the average value of the N/P atomic ratio in Sungo Bay as 4:1, less than the Redfield Ratio of 16:1. Hence, DIN is assumed to be the limiting nutrient in the model. The target species in modeling is kelp. The relationships between the state variables have been studied previously and used in many ecosystem models (e.g., Skogen et al., 1995; Zhao and Guo, 2011). Phytoplankton absorbs DIN for photosynthesis, and releases DIN through respiration. Kelp grows by assimilating DIN. The mortalities of phytoplankton and kelp contribute to POM, which returns to DIN through mineralization. The model includes the variations of the kelp-induced drag during the kelp growth period, and the competition of nutrients between kelp and

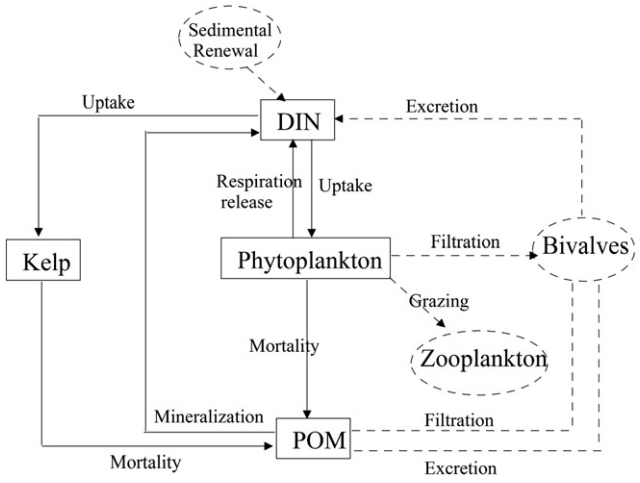

Fig. 7. Conceptual model of the multi-species culture ecosystem in Sungo Bay. The state variables are shown in rectangular boxes and the forcing terms are in dashed ellipses. Solid lines represent the biological processes in the model, and dashed lines represent the processes regarded as external forcing.

phytoplankton. The contribution of bivalves' excretion to DIN flux is considered as a constant source during the growth period of bivalves.

The governing equation of the model state variables is

$$\frac{\partial A}{\partial t} + adv(A) = diff(A) + sources - sinks$$

where A represents a state variable, $adv(A)$ and $diff(A)$ are advection and diffusion driven by the ambient current and mixing. The sources and sinks are different for different state variables, with details provided in Table 1. The corresponding mathematic descriptions of the biological processes are provided in Table 2, and the values of model parameters are given in Table 3 (Duarte et al., 2003; Eppley, 1972; Eppley et al., 1970; Tian et al., 2005; Wu, 2005; Zhang, 2008; Zhao, 2002).

2.4. Model configuration

The model domain leaves an open eastern boundary. The hydrodynamic and aquaculture components are coupled. The model uses the staggered Arakawa-C grids in the horizontal with a resolution of 0.25′×0.25′ in longitude/latitude, and 11 σ-levels in the vertical. The three-dimensional velocity and the state variables in the biological component are updated at the time step of 30 s.

The surface forcing includes the annual cycles of solar radiation (*Rad*, in w m^{-2}) and sea surface temperature (*temp*, in °C), expressed by the following cosine functions of time (t, in Julian day):

$$Rad = 200.38 - 116.47 \times cos[2\pi(t-1)/365],$$

$$temp = 13.1 - 9.2 \times cos\left[2\pi\frac{t-53}{365}\right].$$

The expression for *Rad* is based on Wu (2005); and that for *temp* is based on Kermer (1978).

Based on the Fick's First Law, Cai et al. (2004) reported that the annual mean fluxes of NH_4^+, NO_3^-, NO_2^- from sediment to water column were 376.33, 33.02, 6.41, 10.08 μmol m^{-2} d^{-1}, respectively. In this study, these three components are added together as the flux of DIN from sediment. The rate of the benthic release is set to 415.76 μmol m^{-2} d^{-1}, representing a steady source of nutrient into the bottom grid. The total amount of DIN from the contribution of bivalves' excretion amounts to 278.5 t (Fang et al., 1996c) in regions of bivalves aquaculture (Fig. 3, the bivalve monoculture and the multi-species aquaculture regions) during the period for bivalves aquaculture (from October 1 to May 31 of the following year). The bivalves' excretion provides a continuous source of DIN to the surface layer in the model.

Along the eastern open boundary, the hydrodynamic model is driven by two tidal components, i.e., M_2 and K_1. The tidal harmonic constants are obtained from the Editorial Board for Marine Atlas (1992). The values listed in Table 4 are linearly interpolated to the grids at the open boundary for the calculation of sea level. The boundary conditions for the biological variables are shown in Fig. 8.

Table 1
Model equations for phytoplankton, kelp, particulate organic matter and dissolved inorganic nitrogen.

Phytoplankton (phyt) (mg chl-a m^{-3})	
$\frac{\partial phyt}{\partial t} + adv(phyt) = diff(phyt) + phyt\_gprod - phyt\_resp - phyt\_mort$	
phyt _gprod	: Phytoplankton growth
phyt_resp	: Phytoplankton respiration
phyt _mort	: Phytoplankton mortality
Kelp (g m^{-2})	
$\frac{\partial kelp}{\partial t} = kelp\_gprod - kelp\_mort$	
kelp _gprod	: Kelp growth
kelp _mort	: Kelp mortality
Particulate organic matter (POM) (g m^{-3})	
$\frac{\partial POM}{\partial t} + adv(POM) = diff(POM) + phyt\_mort + kelp\_mort - pom\_minerate * POM$	
pom _minerate	: POM mineralization rate
Dissolved inorganic nitrogen (DIN) (mmol m^{-3})	
$\frac{\partial DIN}{\partial t} + adv(DIN) = diff(DIN) + (phyt\_resp - phyt\_gprod) - kelp\_gprod + pom\_mine + bethic + biv$	
pom _mine	: POM mineralization
bethic	: Benthic release
biv	: Bivalves exudation

Table 2
Mathematic descriptions of the biological processes.

Phytoplankton (phyt)	
$phyt\_gprod = pmax\_phyt \cdot temp\_lim \cdot \min(rad\_lim, din\_lim) \cdot phyt$	
$phyt\_resp = pmax\_phyt \cdot [phyt\_respbas + phyt\_resppho \cdot min(rad\_lim, din\_lim)] \cdot resp\_temp\_lim \cdot phyt$	
$phyt\_mort = phyt\_mortrate \cdot phyt$	
$temp\_lim = e^{al\_temp1 \cdot (temp-10)}$	
$rad\_lim = \frac{I_z}{I_{opt}} e^{\left(1-\frac{I_z}{I_{opt}}\right)}$	
$I_z = I_0 \cdot e^{(k_0 + k_1 \cdot z)}$	
$din\_lim = \frac{DIN}{DIN + k\_DIN}$	
$resp\_temp\_lim = e^{al\_temp2 \cdot (temp-10)}$	
temp _lim	: temperature limitation function of phytoplankton growth
rad _lim	: light limitation function of phytoplankton growth
din _lim	: nutrient limitation function of phytoplankton growth
I_0	: light intensity at surface
I_z	: light intensity at depth z
resp _temp _lim	: temperature limitation function of respiration process
Kelp (g m^{-2})	
$kelp\_gprod = pmax\_kelp \cdot kelp\_temp\_lim \cdot kelp\_din\_lim \cdot kelp$	
$kelp\_mort = kelp\_mortrate \cdot kelp$	
$kelp\_temp\_lim = \frac{2.0 \cdot (1+\beta) \cdot X_t}{X_t^2 + 2.0 \cdot \beta \cdot X_t + 1.0}$	
$X_t = \frac{temp - T_{leth}}{T_{opt} - T_{leth}}$	
$kelp\_din\_lim = \frac{DIN}{DIN + k\_DIN\_kelp}$	
kelp _temp _lim	: temperature limitation function of kelp growth
kelp _din _lim	: nutrient limitation function of kelp growth

Table 3
Parameters used in the aquaculture model of Sungo Bay.

Parameter	Value	Unit	Description of parameter
pmax_phyt	1.2	day^{-1}	Maximum growth rate of phytoplankton
al_temp1	0.055	$(°C)^{-1}$	Temperature-dependent growth rate
I_{opt}	150	W m^{-2}	Optimum light intensity
k_DIN	2.0	mmolN m^{-3}	DIN half saturation constant for phytoplankton
phyt_respbas	0.138	/	Percentage of basic respiration of phytoplankton
phyt_resppho	0.05	/	Percentage of photorespiration
al_temp2	0.054	$(°C)^{-1}$	Temperature-dependent respiration rate
k_0	0.04	/	1# Coefficient of light attenuation
k_1	0.01	/	2# Coefficient of light attenuation
phyt_mortrate	0.05	day^{-1}	Phytoplankton mortality rate
k_NC	12.277	$mmolN(gC)^{-1}$	Ration of N/C in phytoplankton
k_C	50	$mgC(mgChl\text{-}a)^{-1}$	Ration of C/chl-a in phytoplanton
pom_minerate	0.003	day^{-1}	Mineralization rate of POM
POM2N	5.714	$mmolN(gPOM)^{-1}$	Ration of N/POM
pmax_kelp	0.031	day^{-1}	Maximum growth rate of kelp
k_DIN_kelp	1.0	mmolN m^{-3}	DIN half saturation constant for kelp
β	3.0	/	Temperature adjustment parameter for kelp growth
T_{opt}	13	°C	Optimal temperature for kelp growth
T_{leth}	25	°C	Lethal temperature for kelp growth
kelp_mortrate	5.0 10^{-5}	day^{-1}	Kelp mortality rate
kelp2N	1.4%	/	Ration of N/kelp dry weight

Table 4
Tidal harmonic constants used at the open boundary.

Tidal component	Amplitude (cm)	Phase (°)
M_2	50–60	6–36
K_1	25	330

These are combinations of seasonal observations in January, April, July and November of 2006 at the stations located outside the bay (Fig. 1) and data from some previous studies in Sungo Bay (Duarte et al., 2003; Wu et al., 2005; Zhang, 2008). The boundary conditions for biological variables are reconstructed from observations in different years, thus are not representative of any particular year.

The initial currents and sea levels are set to zero. The biological component turns on after the hydrodynamic component has been spun up. The initial fields of phytoplankton (chlorophyll-a), DIN and POM are constructed by interpolating the observed data in November 2006 (Fig. 1). After running the model for one year, the model outputs are used as new initial conditions for subsequent runs. The new initial conditions are less influenced by observational errors and are close to model's climatological state. Fig. 5 shows the raft-culture structure of kelp. The initial weight of the kelp is 1.2 g indiv.$^{-1}$ (Nunes et al., 2003), and the cultivated density is 12 indiv. m^{-2} (Duarte et al., 2003). Consequently, the initial biomass for kelp is 14.4 g m^{-2}. The dry weight of kelp is a state variable calculated in the model, while its length is set to linearly increase from zero on 1st November to 5 m on 31st May of the following year.

3. Results and discussion

3.1. Parameter sensitivity analyses

Model sensitivity experiments are carried out to test how the predicted key variables vary by changing the model parameters within reasonable ranges. The focuses are on the prediction of the annual-mean biomass of phytoplankton and the final production of kelp. Taking the model output and the parameters listed in Table 3 as the control run, the value of any selected parameter is changed and the model is run for one year in each sensitivity experiment. The sensitivity of a predicted state variable to a selected parameter is quantified as

$$S=\left|\frac{\text{change of predicted state variable}}{\text{change of parameter}}\right|.$$

Table 5
Sensitivities of the phytoplankton biomass to the model parameters.

Parameter	Description of parameter	Variation of parameter (%)	Variation of annual phytoplankton biomass (%)	Sensitivity
pmax_phyt	Maximum growth rate of phytoplankton	+50	+15.34	0.33
		−50	−25.59	0.54
phyt_mortrate	Phytoplankton mortality rate	+50	−11.54	0.23
		−50	+40.52	0.81
k_DIN	DIN half saturation constant for phytoplankton	+50	−6.34	0.13
		−50	+4.83	0.10
k_NC	Ration of N/C in phytoplankton	+40	−11.30	0.23
		−50	+17.13	0.34
I_{opt}	Optimum light intensity	+50	−18.80	0.37
		−50	+20.42	0.41
phyt_respbas	Percentage of basic respiration of phytoplankton	+40	−36.80	0.92
		−40	+27.60	0.69
pom_minerate	Mineralization rate of POM	+50	+6.70	0.13
		−50	−6.77	0.14
pmax_kelp	Maximum growth rate of kelp	+5	−13.20	0.26
		−5	+13.20	0.26
k_DIN_kelp	DIN half saturation constant for kelp	+50	+12.56	0.25
		−50	−13.42	0.26
kelp_mortrate	Kelp mortality rate	+50	+1.12	0.02
		−50	−2.29	0.05

Tables 5 and 6 summarize the sensitivity of the annually averaged biomass of phytoplankton and the final output of kelp, respectively. The analyses quantify how one state variable depends on the biological parameters of the other. The annual-mean biomass of phytoplankton is sensitive to the maximum growth rate of kelp ($S=0.26$), while the output of kelp is less sensitive to the maximum growth rate of phytoplankton ($S=0.07$–0.14), because kelp is cultivated in November much earlier than the spring bloom of

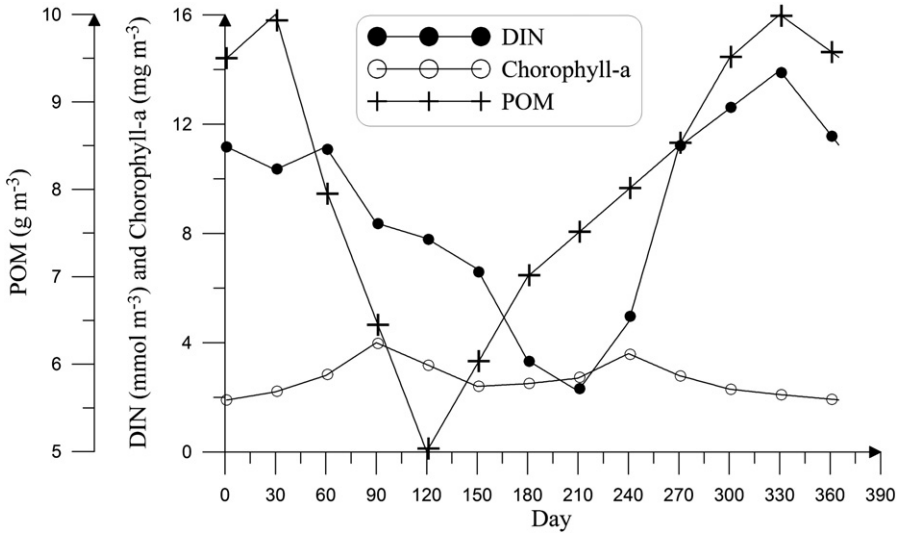

Fig. 8. Annual cycle of biological variables (DIN: dots, mmol m^{-3}; chlorophyll-a: circles, mg m^{-3}; POM: crosses, g m^{-3}) at the mouth of Sungo Bay. The values are based on observations at stations A, B, C and D (Fig. 1) in January, April, July, November 2006, and the previously published data (Duarte et al., 2003; Wu et al., 2005; Zhang, 2008) in order to achieve monthly resolution.

Table 6
Sensitivities of the kelp output to changes to the model parameters.

Parameter	Description of parameter	Variation of parameter (%)	Variation of kelp production (%)	Sensitivity
pmax_phyt	Maximum growth rate of phytoplankton	+50	−3.48	0.07
		−50	+6.91	0.14
phyt_mortrate	Phytoplankton mortality rate	+50	+2.60	0.05
		−50	−2.01	0.04
k_DIN	DIN half saturation constant for phytoplankton	+50	+5.20	0.11
		−50	−7.60	0.15
k_NC	Ration of N/C in phytoplankton	+50	−20.65	0.41
		−50	+12.65	0.32
I_{opt}	Optimum light intensity	+50	+8.26	0.17
		−50	−13.40	0.27
phyt_respbas	Percentage of basic respiration of phytoplankton	+40	+12.87	0.32
		−40	−8.62	0.22
pom_minerate	Mineralization rate of POM	+50	−2.21	0.04
		−50	+1.74	0.03
pmax_kelp	Maximum growth rate of kelp	+5	+17.32	3.46
		−5	−15.61	3.12
k_DIN_kelp	DIN half saturation constant for kelp	+50	−16.54	0.33
		−50	+13.48	0.27
kelp_mortrate	Kelp mortality rate	+50	−2.28	0.05
		−50	+3.79	0.08

phytoplankton. The growth of phytoplankton is significantly influenced by the amount of nutrient left by the early kelp consumption which is determined by the growth rate of kelp. The output of kelp is more sensitive to the respiration rate ($S = 0.22$–0.32) than the growth rate of phytoplankton, because respiration of phytoplankton is an important source of nutrient during the late growth period of kelp when the level of nutrient is low.

The DIN half saturation constants of the phytoplankton and kelp represent their ability to compete for DIN. Smaller DIN half saturation constant means weaker DIN limitation in favor of the growth of a state variable. Hence, increasing in the DIN half saturation constant of kelp leads to decreasing in the output of kelp and increase in the biomass of phytoplankton and vice versa.

3.2. Hydrodynamic field

The key process added to the hydrodynamic model is the influence of aquaculture activities on circulation. To examine the performance of the modified model in predicting flow, the simulated currents in April are compared with the observed currents in April 2006, when the kelp reached the maximum length. Fig. 9 shows the variations of the simulated and observed currents at station 6 (Fig. 1). By integrating the two types of additional drags in the model, both the magnitudes and phases of the flow agree well with the observations.

The vertical profile of the currents in Sungo Bay is very unique and is caused by the suspending aquaculture facilities and species. Fig. 10 compares the simulated currents with and without the aquaculture drags in April and the observed currents in April 2006 at station Xunshan (Fig. 1). By including the obstruction of current related to aquaculture, the simulated current reaches a maximum of 30 cm s^{-1} at 6 m above the bottom, and the results exhibit a good agreement with observations. The thickness of the surface boundary layer caused by the aquaculture activities reaches 6 m and varies regularly with tides. Without the aquaculture drags (Fig. 10c), the model predicts a maximum velocity of 50 cm s^{-1} at the surface, significantly different from the observations.

The tidal flow pattern, following the bathymetry and weakening inshore, is quite robust because it shows up with and without aquaculture. The directions of the currents during flooding and ebbing are similar with and without aquaculture. This indicates that the presence of aquaculture activities have not altered the horizontal pattern of tidal circulation, but causes significant changes in current magnitude. The maximum speeds of the vertically averaged flow are 43 cm s^{-1} and 70 cm s^{-1} with and without the aquaculture drags, respectively. Without aquaculture, the average speeds are 33.1 cm s^{-1}, 19.8 cm s^{-1} and 3.2 cm s^{-1} at the surface, middle, and bottom layers, respectively. By including the aquaculture drags, the

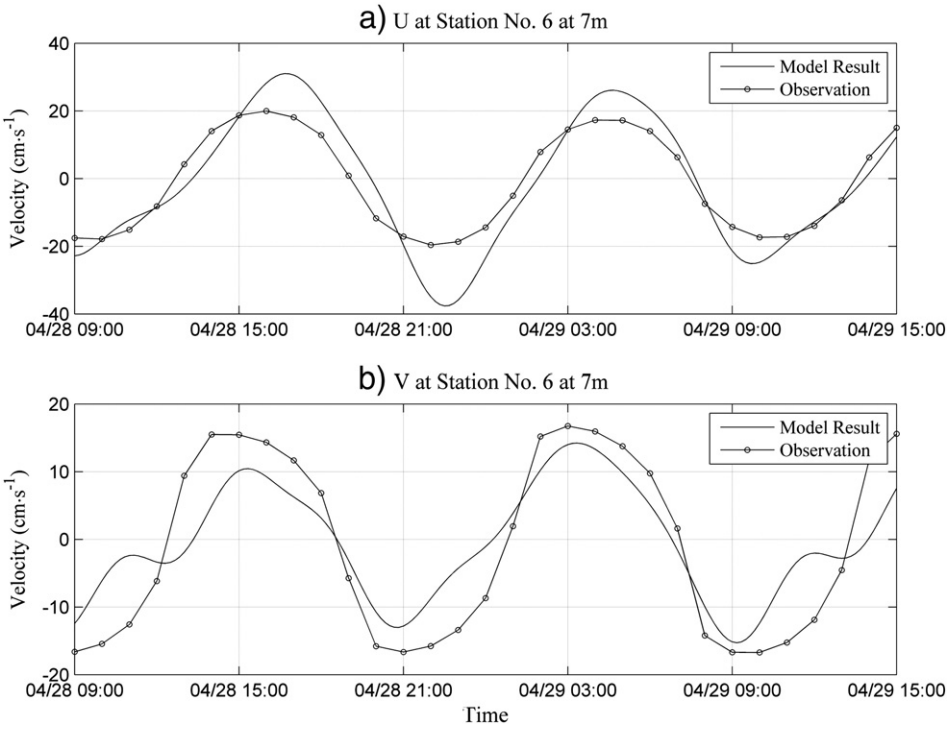

Fig. 9. Comparison between the simulated (solid line) and observed (solid line with circles) currents at station No. 6: (a) east–west component; (b) north–south component (in cm s^{-1}).

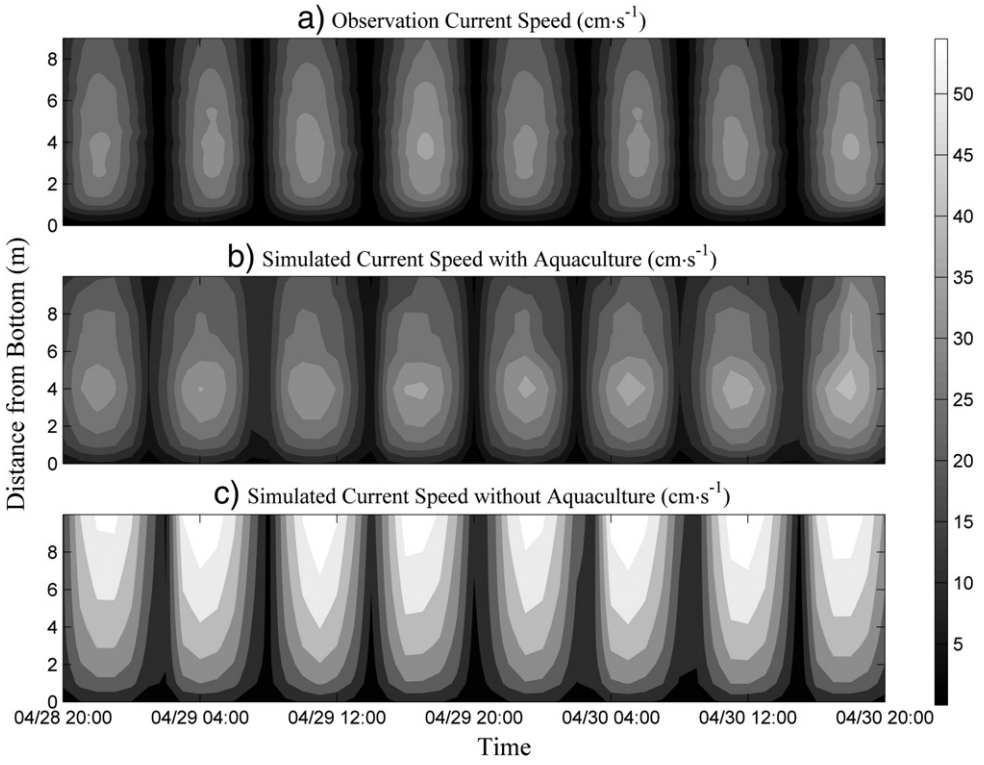

Fig. 10. Depth-time variations of flow speed at station Xunshan, from (a) observations, (b) simulation with aquaculture, and (c) simulation without aquaculture.

corresponding velocities are reduced to 12.2 cm s^{-1}, 13.9 cm s^{-1} and 2.3 cm s^{-1}. Thus the aquaculture facilities and species reduce the average flow speed by 63%. A strong attenuation occurs near the southern side of the mouth and along the north inside of the bay (Fig. 11). Along the mouth of the bay from north to south, the attenuation rate increases from 0.1 to 0.8. In summary, for the simulation of currents in Sungo Bay, neglecting the physical barriers associated with aquaculture will result in significant overestimation of velocity, water exchange rate and nutrient renewal rate.

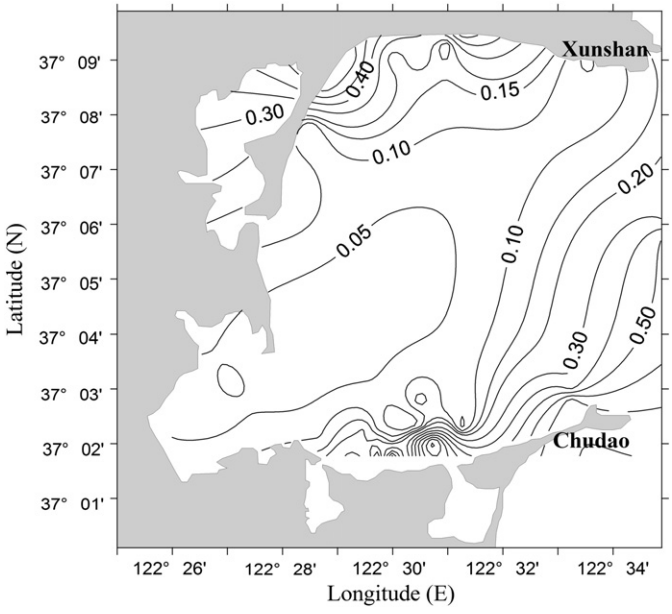

Fig. 11. The attenuation rate of the surface flooding current due to aquaculture.

3.3. Seasonal variations of nutrient

In Sungo Bay, the intensive kelp and bivalves aquaculture over large areas has significant influence on the consumption and production of DIN. Fig. 12 shows the simulated annual cycles of DIN, averaged over the kelp monoculture, bivalve monoculture, and multi-species culture regions. In general, during the kelp growth period from November to May, DIN decreases rapidly due to the assimilation by kelp. After the harvest of kelp in late May, the consumption of DIN by kelp vanishes, while phytoplankton becomes the primary consumer due to the appropriate solar radiation and temperature. As a result, the concentration of DIN remains low until August. From

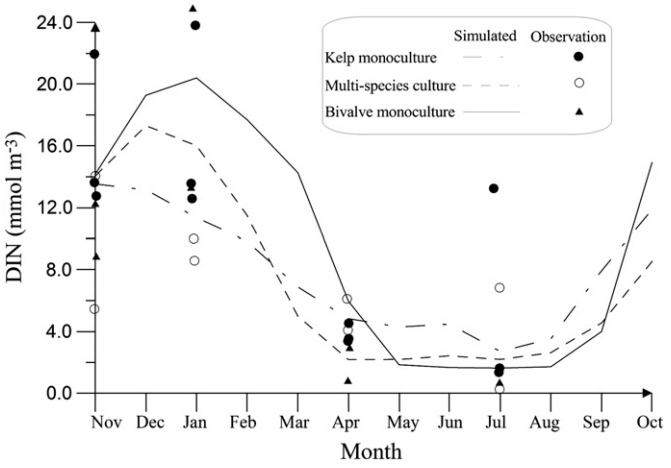

Fig. 12. Simulated and observed annual cycles of DIN averaged in three different aquaculture regions. Solid, dashed and dash–dotted lines represent simulated variations in kelp monoculture, multi-species aquaculture and bivalve monoculture regions respectively. Dots, circles and triangles represent observed values in different regions in January, April, July and November 2006.

September to November before the seeding of kelp, DIN accumulates because kelp is not present and the growth of phytoplankton is limited. Moreover, the model results are generally consistent with the observations.

The variations of DIN concentration in different regions are affected by the different cultivated species. From November to March, the consumption of kelp and the excretion of bivalves are the main sink and source in Sungo Bay, respectively. In the inner part of the bay with bivalve monoculture, the concentration of DIN increases due to the existence of source and the absence of sink. In the kelp monoculture region near the mouth of the bay with sink but without source, the concentration of DIN decreases to the lowest among the three regions. In the multi-species aquaculture region, the excretion of bivalves and assimilation of kelp occur at the same time so the concentration of DIN falls between the values of the other two regions. After March, the limitation on the growth of phytoplankton by temperature and solar radiation weakens and the consumption of phytoplankton becomes another sink of DIN. In the bivalve monoculture region, the early highest level of DIN concentration supports more rapid growth of phytoplankton, and the DIN concentration quickly drops to the lowest level of the three regions. In the kelp monoculture region near the mouth of the bay, the expedite supply of DIN from the open sea makes the DIN concentration reach the highest level of the three regions. After September, the growth of phytoplankton is limited by solar radiation, thus the DIN concentration increases in the whole bay. From October, there is further increase in DIN concentration in regions where the bivalves are cultivated.

According to model simulation, the vertically averaged distribution of DIN concentration in Sungo Bay exhibits obvious seasonal variations and is also influenced by the aquaculture of kelp and bivalves (Fig. 13). In both April and July, the DIN concentration inside the bay is lower than that near the open sea. The region with dense contours in Fig. 13 is the location reached by the water from the open sea. The obvious differences in DIN concentration between April and July are due to the different exchange rates between the bay and the open sea. In April, kelp nearly reaches its maximum length and exerts

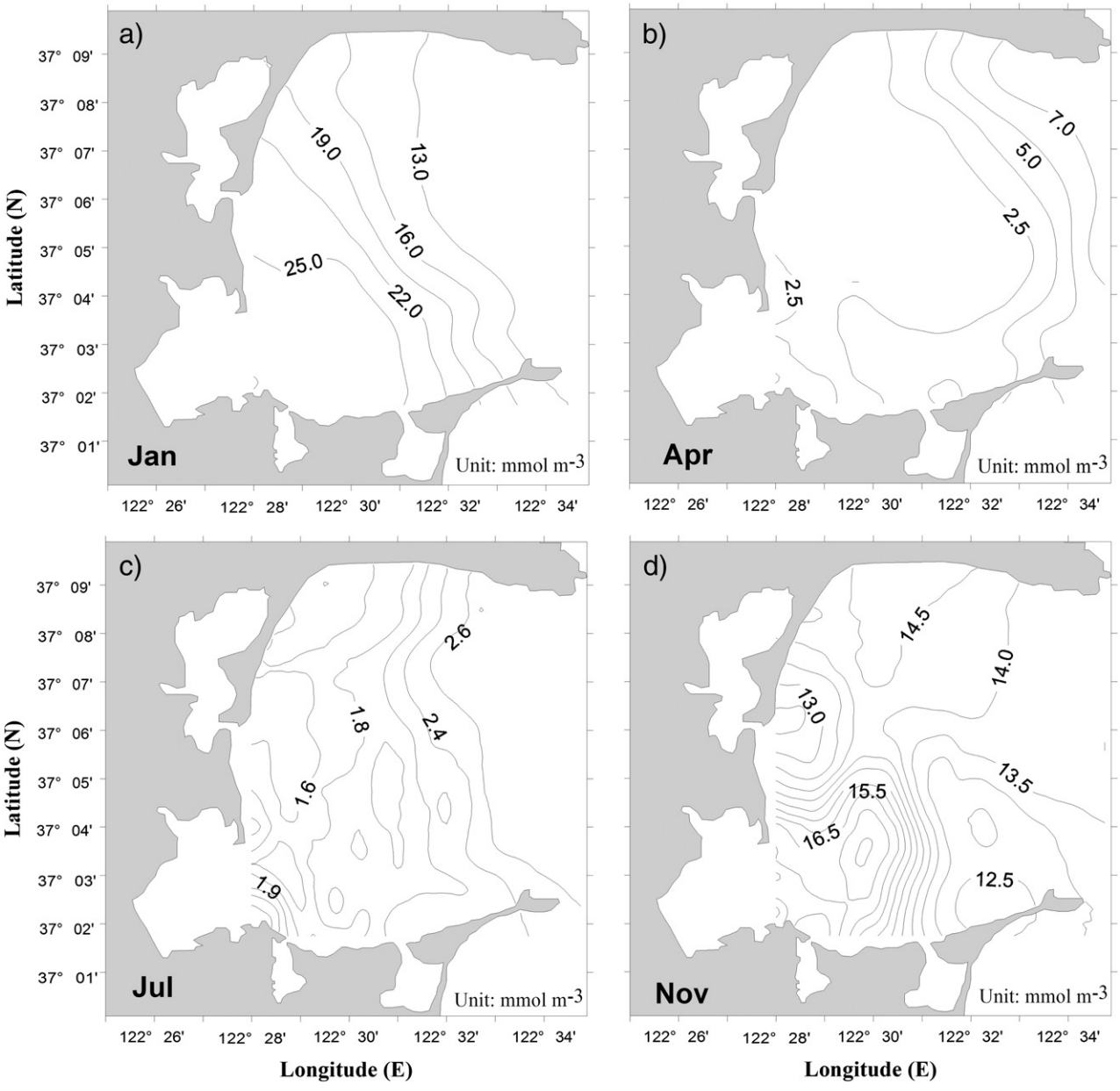

Fig. 13. Simulated vertically averaged distributions of DIN concentration in (a) January, (b) April, (c) July and (d) November, representing winter, spring, summer and autumn, respectively.

the maximum drags on currents. As a result, the DIN supply from the open sea is depleted and higher DIN concentration is only found near the mouth of the bay (indicated by the isoline of 7.0 mmol m^{-3}). In July, kelp and bivalves are totally harvested and the aquaculture drag is only caused by the facilities at surface. The supply of DIN from the open sea can reach the interior of the bay (indicated by the isoline of 2.6 mmol m^{-3}) farther than in April.

Fig. 14a shows the annual DIN budget derived from the model results. Phytoplankton plays an important role in the renewal of DIN. The uptake of DIN through photosynthesis minus the respiration release is an important sink of DIN with an annual net amount of 1013 t. During the growth period, kelp assimilates 981 t of DIN. The supply of DIN from remineralization of POM is 787 t, accounting for 37.7% of the total DIN import. Another important source of DIN is from the open sea. The annual input of DIN through exchange with the Yellow Sea is 700 t, accounting for 33.6% of the total input. The inputs of DIN from benthic release and bivalve excretion are 319 t and 279 t, accounting for 15.3% and 13.4% of the total source, respectively.

During the growth period of kelp (Fig. 14b), DIN supplement from the open sea is 589 t, accounting for up to 84.2% of the annual input from the open sea and 40.2% of the total DIN source during this period. This indicates that the input from open sea is the primary source of DIN for the growth of kelp. During the 210-day growth period of kelp, phytoplankton assimilates 420 t of DIN, accounting for only 41.5% of its total value integrated over one year, possibly due to the competition between kelp and phytoplankton.

3.4. Seasonal variations of phytoplankton

Fig. 15 shows the simulated annual cycle of phytoplankton biomass in Sungo Bay (represented by the concentration of chlorophyll-a). The simulated cycle generally agrees with observations. Phytoplankton biomass increases in spring under favorable temperature and solar radiation, and reaches its maximum in June–July. After July, there are not enough nutrients to support the growth of phytoplankton due to the excessive consumption by both phytoplankton and kelp. The increasing biomass consumes nutrients in the spring whereas the decreasing biomass contributes to nutrients accumulation in autumn. Moreover, the regional differences of phytoplankton biomass are attributed to aquaculture activities. For example, in the kelp monoculture region, kelp competes with phytoplankton. In the bivalve monoculture region, bivalves releases DIN hence promoting the growth of phytoplankton. The phytoplankton biomass is the largest in the bivalve monoculture region, smaller in the multi-species aquaculture region and the smallest in the kelp monoculture region.

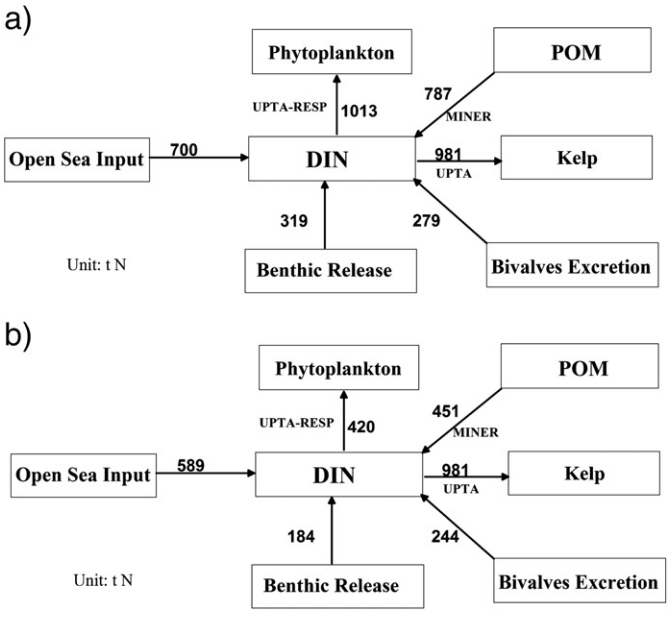

Fig. 14. Simulated nutrient budgets (t N) during (a) the whole year and (b) the growth period of kelp.

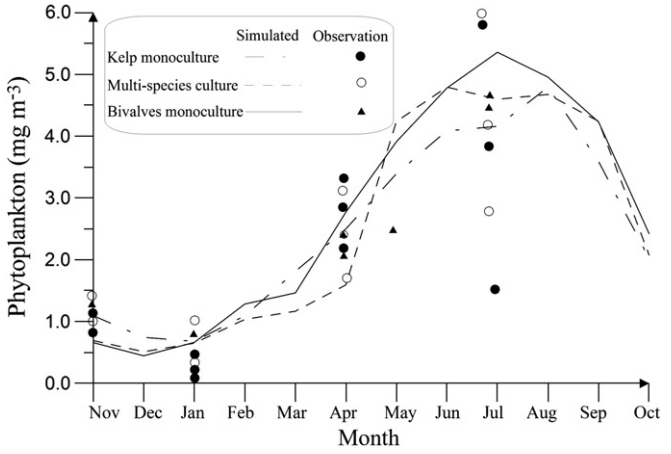

Fig. 15. Simulated and observed annual cycles of phytoplankton biomass averaged in three different aquaculture regions. Solid, dashed and dash–dotted lines represent simulated variations in kelp monoculture, multi-species aquaculture and bivalve monoculture regions respectively. Dots, circles and triangles represent observed values in different regions in January, April, July and November 2006.

3.5. Kelp production

As the primary aquaculture species in Sungo Bay, kelp is usually planted around early November and harvested around late May. Fig. 16 shows the simulated variations of the biomass and the growth speed of kelp. The growth of kelp is mainly controlled by temperature and nutrients. Light is not considered as a limiting factor because the ropes that kelp is fastened to can be adjusted up or down to overcome light limitation. During the growth period of kelp, the water temperature (ranging from 3.9 °C to 22.3 °C) is relatively favorable with the temperature limitation coefficient (*kelp_temp_lim* in Table 2) varying between 0.74 and 1.0. During the early growth period (November to January), the growth of kelp is not much limited by DIN, with the limitation coefficient (*kelp_din_lim* in Table 2) exceeding 0.85. From late January to early March, the biomass of kelp increases faster due to the accumulation in the previous period and consumes more DIN. From March, there are weak limitations on phytoplankton growth by temperature and solar radiation. The growth speed of kelp slows down because of low level of DIN concentration caused by the assimilation of both kelp and phytoplankton.

When harvested, the dry weight of kelp is 7.0×10^4 t according to model results. The actual production in Sungo Bay is about 8.0×10^4 t (Fang et al., 1996a). The difference is due to the exclusion of the kelp cultivated outside of the bay with water depth exceeding 20 m. The open boundary of the model is set near the mouth of the bay because of the lack of observations away from the mouth. In the following discussion on the carrying capacity of kelp, the region outside the bay is not considered.

Fig. 17 shows the distribution of kelp production, i.e., the biomass on May 31st before the final harvest of kelp. In the kelp aquaculture region, the distribution was not uniform. The biomass decreased from the mouth of the bay to the interior. The dry weight has the highest value of 2248 g m^{-2} near the mouth of the bay, about 700 g m^{-2} in the multi-species aquaculture region, and has the lowest value of 271 g m^{-2} in the interior of the bay. The distribution is associated

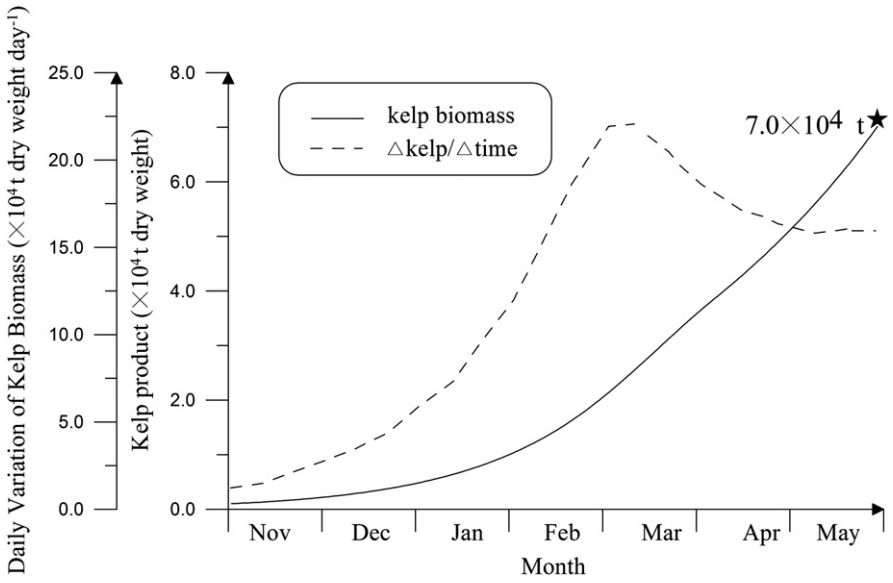

Fig. 16. Simulated variations of kelp biomass (solid line, $\times 10^4$ t dry weight) and growth rate (dashed line, $\times 10^4$ t dry weight day^{-1}).

with different DIN supplies from the open sea, which are an important factor influencing the growth of kelp. In the late growth period, the DIN concentration is very low inside of Sungo Bay due to the assimilation of both phytoplankton and kelp that makes the supply from the open sea even more important. Near the mouth of the bay, the water exchange rate is high, allowing sufficient supply of DIN for kelp thus resulting in a high production. From the mouth to the end of the bay, the aquaculture facilities and kelp slow down the tidal current, and consequently obstruct the transport of nutrient.

3.6. Preliminary estimation of kelp carrying capacity

Model results suggest that the exchange with the open sea is the main nutrient source supporting the growth of kelp. Aquaculture facilities at the surface and kelp in the water column act as drags on the current and thus reduce the exchange rate with the open sea. If the aquaculture density is increased, kelp will deplete DIN quickly and the increased drags will reduce the DIN supply inside the bay, and thus limit the growth of kelp. If the aquaculture density is decreased, there will be less drag and more DIN supply. But if nutrient supply is sufficient, less kelp seeded leads to less harvest. The relationship among the aquaculture density, the exchange rate with the open sea and the final production determines an optimal density corresponding to the maximum production, i.e. the carrying capacity of kelp.

Numerical experiments with different aquaculture densities of kelp are carried out to search for the optimal aquaculture density. Table 7 lists the initial values of kelp and values of two types of aquaculture drag coefficients used in this set of simulations. The numerical experiments are denoted by DENSITY_0.8, DENSITY_0.9, DENSITY_1.1, DENSITY_1.2 and DENSITY_1.5, with the initial kelp

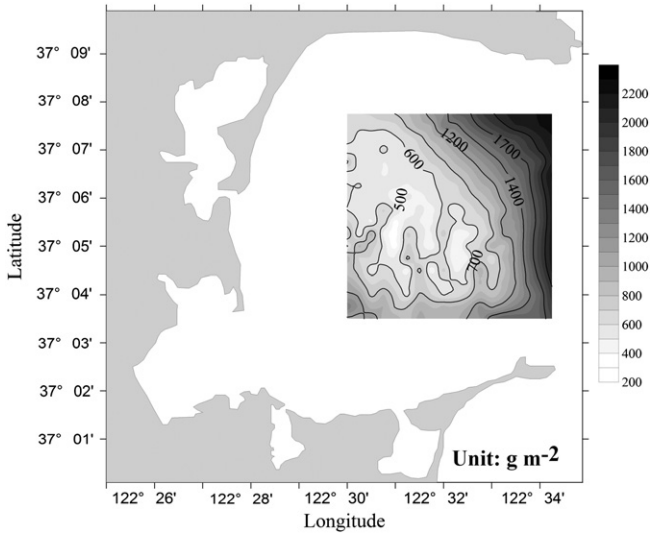

Fig. 17. Simulated distribution of the kelp production (biomass in May 31).

Table 7
Initial conditions of kelp and values of the aquaculture drags in five numerical experiments.

Experiment name	Initial value of kelp (g/m^2)	Surface drag coefficient (C_{ds})	Drag coefficient in the water column (C_D)
CONTROL	14.4	0.07	0.025
DENSITY_0.8	14.4×0.8	0.07×0.8	0.025×0.8
DENSITY_0.9	14.4×0.9	0.07×0.9	0.025×0.9
DENSITY_1.1	14.4×1.1	0.07×1.1	0.025×1.1
DENSITY_1.2	14.4×1.2	0.07×1.2	0.025×1.2
DENSITY_1.5	14.4×1.5	0.07×1.5	0.025×1.5

Table 8
Results of current velocity, DIN supply from the open sea and the corresponding kelp production in five numerical experiments.

Experiment name	Velocity in kelp culture region		DIN supply from the open sea		Kelp production	
	Estimates (cm/s)	Deviation from CONTROL	Estimates (t N)	Deviation from CONTROL	Estimates ($\times 10^4$ t)	Deviation from CONTROL ($\times 10^4$ t)
CONTROL	10.80	/	589.17	/	7.01	/
DENSITY_0.8	12.13	+12.3%	721.74	+23%	6.76	−0.25
DENSITY_0.9	11.42	+5.8%	661.13	+12%	7.21	+0.20
DENSITY_1.1	10.26	−5.0%	555.22	−6%	7.08	+0.07
DENSITY_1.2	9.78	−9.5%	510.10	−13%	6.80	−0.21
DENSITY_1.5	8.61	−20.3%	397.91	−32%	6.39	−0.62

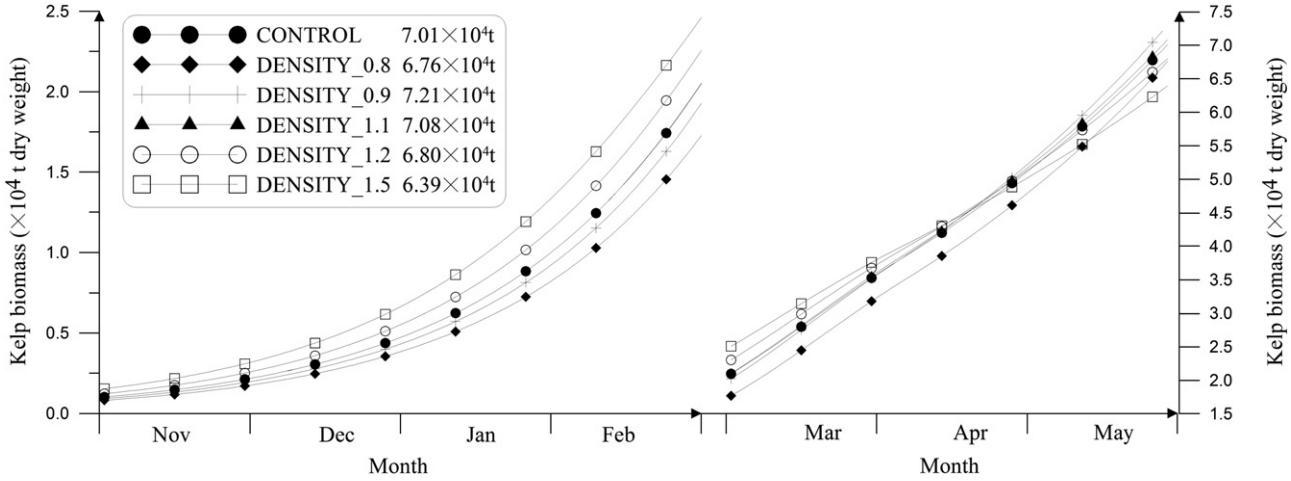

Fig. 18. Simulated variations of kelp biomass under different aquaculture densities.

densities set to be 0.8, 0.9, 1.1, 1.2 and 1.5 times of that in practice now (CONTROL run). The aquaculture drag coefficients are set to be proportional to the aquaculture density.

Table 8 shows the magnitude of current, DIN supply and the final production of kelp obtained by different experiments. As the aquaculture density is increased to 1.1, 1.2 and 1.5 times the current value, the average velocity in kelp aquaculture region decreases by 5.0%, 9.5% and 20.3% respectively. On the other hand, by decreasing the aquaculture density to 0.9 and 0.8 times of the current value, the average velocity increases by 5.8% and 12.3%, respectively. Correspondingly, the DIN supply from the open sea changes by 23%, 12%, −6%, −13% and −32% as the aquaculture density changes from 0.8, 0.9, 1.1, 1.2 and 1.5 times of the current value. The final production of kelp does not change monotonically, because the two determining factors (aquaculture density and DIN supply) have opposite trends. Fig. 18 shows the time-variation of kelp biomass for different aquaculture densities. From November to late February, the kelp biomass is larger as the aquaculture density increased because of the sufficient DIN during this period. From early March to the harvest period, the variation in kelp biomasses is more complex. The nutrient demand is greater for higher aquaculture density but the DIN supply from the open sea is impeded more severely. As a result, the maximum kelp production does not occur when the aquaculture density is highest. Model results suggest that the optimal aquaculture density is 0.9 times of the current value and the corresponding maximum final production is 7.2×10^4t in dry weight. This is the carrying capacity of kelp determined by this model.

The present study is a preliminary step to find the optimal average aquaculture density. In fact, determining the carrying capacity of kelp is a complicated issue, because there are many influencing factors. Carrying capacity may be not spatially uniform because DIN supply from the open sea depends on variations in water exchange rates. Theoretically, the optimal aquaculture density decreases from the mouth to the end of the bay. However, higher density near the mouth causes more severe obstruction on current, thus reduces the DIN supply to the inner region and the kelp production there. Thus, reducing the density near the mouth may help to increase the overall production. This has been tested by additional simulation in which only the density near the mouth of the bay was reduced to 0.9 times of the current value. The production of kelp increases to 7.32×10^4t in dry weight, higher than that obtained by other simulations specifying uniform density. In addition, the aquaculture of bivalves also plays an important role on the carrying capacity of kelp. Bivalves have been successfully cultivated alongside with kelp since the excretion of bivalves acts as a source of DIN (Fang et al., 1996d), and such multi-species aquaculture helps to increase the carrying capacities. Other dynamic processes such as wind and wave can influence the benthic release of DIN through enhancing mixing, and thus result in changes in the carrying capacity.

4. Conclusions

Sungo Bay is a typical area for multi-species aquaculture on the coast of northern China. Both kelp and bivalves are suspended on rafts in the water. Considering the importance of the obstruction of aquaculture activities on hydrodynamics, the parameterization of two types of aquaculture drags caused by aquaculture facilities at the surface and kelp in the water column is introduced into a three-dimensional aquaculture model. The model results well reproduce the unique vertical structure of currents in suspended aquaculture site and show a 40% reduction in the average flow speed. This approach obviously provides a more accurate estimation of current field for driving the transport of DIN and phytoplankton. As expected, the simulated spatial and temporal variations of DIN and phytoplankton are controlled by the distribution of aquaculture species. The aquaculture density of kelp and the DIN supply from the open sea have opposite influences on the kelp production. Model experiments are carried out to explore the existence of an optimal aquaculture density corresponding to the maximum production. The optimal average aquaculture density of kelp is obtained, i.e., about 0.9 times of the current aquaculture density.

As consideration for future work, bivalves need to be integrated into the model as a state variable, because scallops and oysters are not only important economic species in Sungo Bay but also the crucial components in the polyculture system in which the growth of different species depend highly on each other. When estimating aquaculture carrying capacity, there may be an optimal spatial distribution of different species that enables the maximum yield.

Acknowledgments

This research is funded in part by the Chinese Ministry of Science and Technology under the contract 2006CB400602, the National Natural Science Foundation of China under the contract 40830854, the Specialized Research Fund for the Doctoral Program of Higher Education (SRFDP) under the contract 20100132120015 and the Fundamental Research Funds for Central Universities of the Ministry of Education of China under the contract 201013031. We thank three anonymous reviewers and Dr. Youyu Lu for helpful comments on the original manuscript.

References

Bachelor, G.K., 1967. An Introduction to Fluid Dynamics. Cambridge University Press, New York, p. 615.

Bacher, C., Duarte, P., Ferreira, J.G., Héral, M., Raillard, O., 1998. Assessment and comparison of the Marennes-Oléron Bay (France) and Carlingford Lough (Ireland) carrying capacity with ecosystem models. Aquat. Ecol. 31, 379–394.

Boyd, A.J., Heasman, K.G., 1998. Shellfish mariculture in the Benguela System: water flow patterns within a mussel farm in Saldanha Bay, South Africa. J. Shellfish Res. 17, 25–32.

Cai, L.S., Fang, J.G., Dong, S.L., 2004. Preliminary studies on nitrogen and phosphorus fluxes between seawater and sediment in Sungo Bay. Marine Fisheries Research 25, 57–64 (in Chinese with an English abstract).

Duarte, P., Meneses, R., Hawkins, A.J.S., Zhu, M., Fang, J., Grant, J., 2003. Mathematical modeling to assess the carrying capacity for multi-species culture within coastal waters. Ecol. Model. 168, 132–147.

Editorial Board for Marine Atlas (Chief Editor, Chen, D. X.), 1992. Marine Atlas of Bohai Sea, Yellow Sea, East China Sea: Hydrology, China Ocean Press, Beijing.

Eppley, R.W., 1972. Temperature and phytoplankton growth in the sea. Fish Bull 1063–1085.

Eppley, R.W., Reid, F.M.H., Strickland, J.D.H., 1970. Estimates of phytoplankton crop size, growth rate and primary production. In: Strick, l, J.D.H. (Eds.), The Ecology of Plankton Off La Jolla, California, in the Period April through September 1967, 17. Bull. Scripps Inst. Oceanogr, pp. 33–42.

Fan, X., Wei, H., Yuan, Y., Zhao, L., 2009. Vertical structure of tidal current in a typically coastal raft-culture area. Cont. Shelf Res. 29, 2345–2357.

Fang, J.G., Sun, H.L., Kuang, S.H., Sung, Y., Zhou, S.L., Song, Y.L., Cui, Y., Zhao, J., Yang, Q.F., Li, F., 1996a. Assessing the carrying capacity of Sungou Bay for culture of kelp *Laminaria Japonica*. Mar. Fisheries Res. 17, 7–17 (in Chinese with an English abstract).

Fang, J.G., Kuang, S.H., Sun, H.L., Sun, Y., Zhou, S.L., Song, Y.L., Cui, Y., Zhao, J., Yang, Q.F., Li, F., 1996b. Study on the carrying capacity of Sungou Bay for the culture of scallop *Chlamys Farreri*. Mar. Fisheries Res. 17, 18–31 (in Chinese with an English abstract).

Fang, J.G., Kuang, S.H., Sun, H.L., Li, F., Zhang, A.J., Wang, X.Z., Tang, T.Y., 1996c. Mariculture status and optimizing measurements for the culture of scallop *Chlamys Farreri* and kelp *Laminaria Japonica* in Sungou Bay. Mar. Fisheries Res. 17, 95–102 (in Chinese with an English abstract).

Fang, J.G., Sun, H.L., Yan, J., Kuang, S.H., Feng, L., Hewkirk, G.F., Grant, J., 1996d. Polyculture of scallop *Chlamys farreri* and kelp *Laminaria Japonica* in Sungo Bay. Chin. J. Oceanol. Limnol. 14, 322–329.

Gibbs, M.M., James, M.R., Pickmere, S.E., Woods, P.H., Shakespear, B.S., Hickman, R.W., Illingworth, J., 1991. Hydrodynamics and water column properties at six stations associated with mussel farming in Pelorus Sound, 1984–85. N.Z. J. Mar. Freshwater Res. 25, 239–254.

Grant, J., 1996. The relationship between bioenergtics and the environment to the field growth of cultured bivalves. J. Exp. Mar. Biol. Ecol. 200, 239–256.

Grant, J., Bacher, C.A., 2001. A numerical model of flow modification induced by suspended aquaculture in a Chinese Bay. Can. J. Fish. Aquat. Sci. 58, 1003–1011.

Grant, J., Stenton-Dozey, J., Monteiro, P., Pitcher, G., Heasman, K., 1998. Shellfish culture in Benguela system: a carbon budget of Saldanha Bay for raft culture of *Mytilus galloprovincialis*. J. Shellfish Res. 17, 41–49.

Grant, J., Curran, K.J., Guyondet, T.L., Tita, G., Bacher, C., Koutitonsky, V., Dowd, M., 2007. A box model of carrying capacity for suspended mussel aquaculture in Lagune de la Grande-Entrée, Iles-de-la-Madeleine, Québec. Ecol. Model. 200, 193–206.

Jackson, G.A., Winant, C.D., 1983. Effect of a kelp forest on coastal currents. Cont. Shelf Res. 2, 75–80.

Kashiwai, M., 1995. History of carrying capacity concept as an index of ecosystem productivity. Bull. Hokkaido. Natl. Fish. Res. Inst. 59, 81–101.

Kermer, N., 1978. Coastal Marine Ecosystem. Springer, Berlin.

Nunes, J.P., Ferreira, J.G., Gazeau, F., Lencart-Silva, J., Zhang, X.L., Zhu, M.Y., Fang, J.G., 2003. A model for sustainable management of shellfish polyculture in coastal bays. Aquaculture 219, 257–277.

Pilditch, C.A., Grant, J., Bryan, K.R., 2001. Seston supply to sea scallops (*Placopecten magellanicus*) in suspended culture. Can. J. Fish. Aquat. Sci. 25, 241–253.

Raillard, O., Ménesguen, A., 1994. An ecosystem box model for estimating the carrying capacity of a macrotidal shellfish system. Mar. Ecol. Prog. Ser. 115, 117–130.

Skogen, M.D., Svendsen, E., Berntsen, J., Aksnes, D., Ulvestad, K.B., 1995. Modelling the primary production in the North Sea using a coupled three-dimensional physical–chemical–biological ocean model. Estuarine Coast. Shelf Sci. 41, 545–565.

Tian, T., Wei, H., Su, J., Ghung, C., 2005. Simulation of annual cycle of phytoplankton production and the utilization of nitrogen in the Yellow Sea. J. Oceanogr. 61, 343–357.

Wildish, D., Kristmanson, D., 1997. Benthic Suspension Feeders and Flow. Cambridge University Press, New York.

Wu, J.X., 2005. Development and applications of dynamic model for dissolved nitrogen and phosphate budgets in Sungo Bay, Thesis of Master degree. (in Chinese with an English abstract).

Wu, J.X., Sun, Y., Zhang, Q.Q., Wang, X.L., 2005. Research on the exchange rates of TOC, TN, TP at the sediment–water interface in aquaculture water areas of Sungo Bay. Mar. Fisheries Res. 26, 62–67 (in Chinese with an English abstract).

Zhang, J.H., 2008. Effect of filter feeding shellfish mariculture on the ecosystem and the evaluation of ecology carrying capacity, Thesis of Doctor degree. (in Chinese with an English abstract).

Zhao, L., 2002. A modeling study of the phytoplankton dynamic in the Bohai Sea. Thesis of Doctor degree. (in Chinese with an English abstract).

Zhao, L., Guo, X.Y., 2011. Influence of cross-shelf water transport on nutrients and phytoplankton in the East China Sea: a model study. Ocean Sci. 7, 27–43.

Zhu, M.Y., Zhang, X.L., Tang, T.Y., Ferreira, J.G., Fang, J.G., Wang, X.Z., 2002. Application of ecological model in studying the sustainable development of coastal shellfish culture. Adv. Mar. Sci. 20, 34–42.